Heliyon 9 (2023) e13958

Contents lists available at ScienceDirect

Heliyon

journal homepage: www.cell.com/heliyon

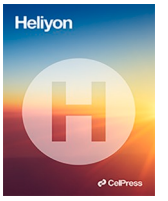

Research article

Intra-source provenance study on Monte Arci (Sardinia) obsidian by pXRF: Role of the data acquisition and analysis tools

Valentina Mameli [a,b,*], Marco Sanna Angotzi [a,b], Emanuele Farinini [c], Riccardo Leardi [c], Carlo Lugliè [d], Carla Cannas [a,b,**]

[a] Department of Chemical and Geological Sciences, University of Cagliari, Monserrato CA, Italy
[b] Consorzio Interuniversitario Nazionale per la Scienza e Tecnologia dei Materiali (INSTM), Cagliari Unit, Italy
[c] Department of Chemistry and Industrial Chemistry, University of Genoa, Italy
[d] Department of Humanities, Languages and Cultural Heritage, University of Cagliari, Cagliari, Italy

ARTICLE INFO

Keywords:
Natural glass
Western Mediterranean
X-ray fluorescence
Chemometrics
Multivariate analysis

ABSTRACT

In this work, a detailed study of Monte Arci obsidian sub-sources using the increasingly accessible technique of pXRF is presented based upon a large dataset of 68 geological samples, for the development of X-ray fluorescence-based analytical standardless procedure. In addition, a non-conventional (for obsidian provenance study) direct application of multivariate analysis on XRF spectra (continuous variables), rather than absolute concentrations or intensity ratios (discrete variables) is proposed.

Results from different softwares and data analysis approaches (bi-/trivariate *versus* multivariate) were compared. In a blind test, the bi-/trivariate approach led to the correct assignment for the main SA, SB, and SC sub-sources, taking into account averaged values of intensity ratios with their standard deviation obtained from three independent measurements. A high intra-source variability for the SB subgroups was detected (almost 13% of error in the assignment, 9 samples out of 68). A non-conventional application of multivariate analysis was carried out directly on the XRF spectra and correct assignments were obtained for SA, SB1, SC groups, while 71% of the SB2 samples were correctly identified. The non-destructive analysis on 14 archaeological samples from Su Carroppu (Carbonia, southwestern Sardinia) rockshelter and from the Middle Neolithic (MN) 422 structure of the open-air dwelling site at Cuccuru is Arrius (Cabras, central-western Sardinia) permitted to test the method and hypothesise their provenance. The comparison with visual characterization or previous analyses by Particle Induced X-Ray Emission (PIXE) permitted to verify the correct provenance assignment of all artifacts for the bi-/trivariate method, and for 12/14 samples in the case of the multivariate one. The standardless analytical approach proposed in this work can represent a more general method exploitable for other obsidian sources, other glassy materials, besides other materials of archaeological interest.

1. Introduction

Obsidian is a raw material produced by fast cooling of acidic lavas [1] that can be defined as a composite where a predominant

* Corresponding author. Department of Chemical and Geological Sciences, University of Cagliari, Monserrato CA, Italy.
** Corresponding author. Department of Chemical and Geological Sciences, University of Cagliari, Monserrato CA, Italy.
E-mail addresses: valentina.mameli@unica.it (V. Mameli), ccannas@unica.it (C. Cannas).

https://doi.org/10.1016/j.heliyon.2023.e13958
Received 17 December 2022; Received in revised form 16 February 2023; Accepted 17 February 2023
Available online 23 February 2023

glassy matrix coexists with microphenocrysts of different crystalline phases, even nanostructured, leading to a variety of morphologies and magnetic behaviours [2–37].

Since the Stone Age in Africa and Middle Palaeolithic in Eurasia, due to its mechanical properties (*i.e.* excellent workability and conchoidal fracture), and optical properties, obsidian has been used for the production of both everyday-life tools and objects of symbolic value [1,38]. In prehistory, obsidian has been preferably exploited even in places where alternative materials were available and exchange networks have been established in time [38]. Indeed, sources of obsidian are limited in number and often located far away from the archaeological sites where the artifacts are discovered [26]. This aspect has represented the ideal premise for the archaeologists to reconstruct the routes of obsidian circulation and subsequently the social and economic organisation of the ancient communities and their interactions by means of provenance studies, based on the assignment of each artefact to the outcrop [26,39,40]. Indeed, each obsidian source has its own geological history for both thermodynamic and cooling conditions, which has produced specific chemical, physical and structural features [16]. Therefore, a different chemical composition depending on the provenance (a sort of geo-chemical signature) can be identified [40]. The case of the Western Mediterranean, where besides a single mainland late Pleistocene case in south-eastern Spain [41], the unique obsidian sources used since the VI millennium B.C. are located in four Italian islands (Lipari, Palmarola, Pantelleria, and Sardinia), indicates a strong motivation and seafaring abilities of Neolithic humans [38].

In the literature, different analytical methods, both destructive and non-destructive, have been proposed with the aim of discriminating the main sources and intra-source variability of obsidian on the basis of its geo-chemistry, physical properties, or geological age [42]. It is worth noting that, among all these methods, non-destructive approaches are requested to preserve artifacts. Moreover, another important aspect to keep in mind is the so-called provenance postulate proposed by Weigand in 1977 [43] and reworded by Neff in 2000 [44] as follows: "*Sourcing is possible as long as there exists some qualitative or quantitative chemical or mineralogical difference between natural sources that exceeds the qualitative or quantitative variation within each source*" [45]. These studies were first conducted by wholly or partially destructive techniques on a few samples and without an in-depth analysis of technological aspects as the position/status in the *raw material reduction trajectory*. On the contrary, today, analytical and archaeological issues are considered according to an integrated approach. For this reason, the analysis, preferably by non-destructive methods, of several samples is fundamental. It arises from this discussion the necessity of routinal non-destructive characterisation methods [42].

The first provenance studies on the Mediterranean obsidian following analytical methods, dated back to the '60s, were carried out by Cann and Renfrew by optical emission spectroscopy, based on differences on the ppm contents of various elements as Ba, Zr, Nb, and Y. Two Monte Arci sub-sources were identified but not localised [46]. To date, among the different Monte Arci outcrops [47] four geo-chemical groups are considered to be relevant for provenance studies [48], namely: SA, SB1, SB2, and SC. From the '60s until today, the elemental analyses on Monte Arci obsidian have been based principally on Neutron Activation Analysis (NAA) [49–54], Particle Induced X-Ray Emission (PIXE) [48,55–63], microanalysis by scanning electron microscopy (SEM-EDS) [20,25,64–67], and X-Ray Fluorescence (XRF) [40,47,68–87]. Other studies were based on infrared [88] and Raman spectroscopy [88], prompt gamma activation analysis [88], magnetometry [33,89], and ^{57}Fe Mössbauer spectroscopy [3,18,90].

Among the XRF-based studies (Table S1), some aimed in distinguishing among the Western Mediterranean obsidian sources [40,47,68,71,73–75,78,79], or focused on Monte Arci sub-sources discrimination [40,47,69,70,72–74,76–78,81–87]. The number of geological samples analysed by XRF was lower or equal to 25 in some studies [68,71,73,79,81] and between 35 and 60 in the other references [47,70,72,74,77,78]. Most of the analytical methods are based on the use of absolute concentrations [40,68,70–72,75–78], obtained based on the calibration of the intensities through the analysis of reference materials, *i.e.* international rock standards. On the contrary, Terradas *et al.* [73] proposed the use of intensities normalised for the emission line of the source, while Acquafredda *et al.* [79] used the intensity ratios. Only in a few of these works multivariate analysis by principal component analysis [68,74] or hierarchical clustering analysis [68] was adopted to treat the extracted XRF data on Monte Arci obsidians. In particular, Orange *et al.* [74] showed the clustering of 24 geological samples from Monte Arci, Palmarola, and Pantelleria by a PCA, where SA and SC groups featured higher absolute values of Zn and Sr, respectively. The multivariate analysis proposed by Kasztovszky *et al.* revealed that Sardinia obsidian samples did not form a definite cluster [68].

In this study, the Monte Arci intra-source provenance issue is tackled on the basis of a standardless *p*-XRF-EDS approach, by selecting the best experimental conditions and evaluating the data by different softwares (LabLithos, Origin, PyMca) and analysis approaches (*i.e.*, bi-/trivariate *versus* multivariate analyses), in order to set up a non-destructive, time-, and cost-effective archaeometric routine and highlight possible issues related to intra-sample, and intra-source variabilities. Both geological (68 samples) and archaeological (14) samples were analysed, with the geological ones in form of powdered and intact samples. The bi-/trivariate plots were obtained based on intensity ratios for different Kα lines, while multivariate analysis was applied directly to the XRF spectra.

2. Materials and methods

2.1. Obsidian geological samples

The geological samples were sourced in the four outcrops of Monte Arci and georeferenced by C. Lugliè [48]. 11 samples were analysed by pXRF as powder, 5 samples as both intact and powder. These samples were previously characterised [37] and their provenance was known and GPS recorded (Table S2). The powders were obtained by hand-milling through an agate mortar and pestle to avoid possible metal contamination. Additionally, 68 samples were analysed as intact and their provenance was communicated by C. Lugliè once the assignment to the geo-chemical group was hypothesised based on the XRF data. The location of the geological sampling areas is shown in Fig. 1.

2.2. Obsidian archaeological samples

Fourteen artifacts coming from the Early Neolithic (EN) phase of the Su Carroppu (Carbonia, south western Sardinia) rockshelter [60] (CAR01-CAR10) and four from the Middle Neolithic (MN) 422 structure of the open-air dwelling site at Cuccuru is Arrius (Cabras, central-western Sardinia, Fig. 1) [91] were analysed non-destructively by pXRF (Fig. S1). The artifacts were selected considering that the archaeological sites are representative of the so-named Monte Arci obsidian "contact zone" and "direct procurement zone" [39], since they are about 65 and 20 km far from the volcanic massif, respectively. Su Carroppu dates back to the mid of the VIth millennium BCE and the EN lithic assemblage is for the biggest part (82%) made of obsidian. The backfilling of the Cuccuru is Arrius 422 pit structure, on the other hand, spans the second quarter of the Vth millennium BCE. During this phase the frequentation of this structure belongs exclusively to the regional Bonu Ighinu culture and obsidian accounts for about 93% of the lithic industry there.

2.3. Portable X-ray fluorescence (pXRF)

X-ray Fluorescence (XRF) spectra were recorded by the portable LITHOS spectrophotometer from ASSING S.p.A. (Fig. S2), equipped with a Mo X-ray source and an EDS detector with a resolution of 160 eV and cooled by Peltier effect. The instrument was previously used in order to study the provenance of menhir statues from Sardinia [92,93]. The spectra were acquired at 25 kV and 0.150 mA. The instrument works in a fixed geometry with angle of 45°, in a non-contact mode. A laser interferometer and a CCD camera, included in the analytical head of the spectrophotometer, permitted to set the sample surface at the analysis distance of 10 mm (along *z* axis). The laser interferometer allowed also the selection of the analysed area (in the *x-y* plane) on the sample. Its size can be

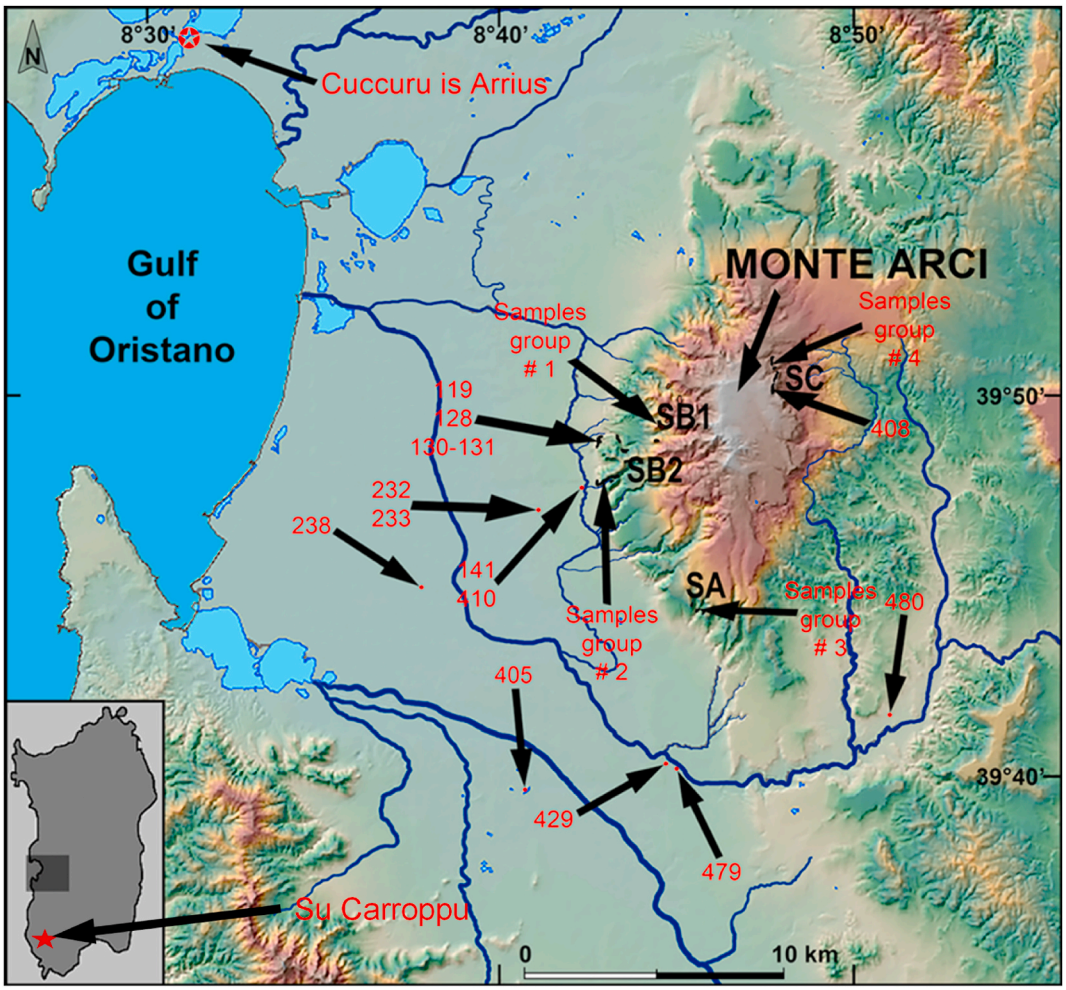

Fig. 1. Location of the geological sampling areas and the archaeological site of Cuccuru is Arrius (Cabras, central-western Sardinia). Group 1: N104, 109, 222, 223, 224, 225, 226, 228, 230, 231, 516, 517, 518, 519, 520, 521, 522; Group 2: N119, 126, 127, 128, 211, 212, 213, 216, 217, 353, 354, 355, 356, 357, 358, 509, 510, 511, 512, 513, 514, 515; Group 3: N132, 133, 134–135, 147–148, 149–150, 151–152, 409, 425, 426, 481, 499, 500, 501, 502, 503, 504, 505, 506, 507, 508; Group 4: N489, 490, 491, 492, 493, 494, 495, 496, 497, 498. The archaeological site of Su Carroppu (Carbonia, southwestern Sardinia) is indicated in the inset in the south-west compared to Monte Arci massif.

decided according to different beam shutters of different diameters (Fig. S3). A zirconium filter is also present to reduce the light elements contribution. The analysis time can be also chosen (Fig. S4).

Each powdered obsidian sample was pressed on a plexiglass sample holder to expose a planar surface to the X-ray beam, and one spectrum was acquired. On each intact sample, three independent measurements on three different zones were acquired. In addition, on the sample N408 for each area analysed by pXRF two additional measurements were acquired under the same experimental conditions to have triplicates for each of the three different analysed zones, in order to estimate the repeatability of the method (for a total of 9 measurements).

2.4. Curve fitting

The XRF spectra were fitted by using different software for comparison: a common software for the data analysis (Origin), the software of the instrument (LabLithos) and a specific software for the visualization and analysis of energy-dispersive X-ray fluorescence data developed by the Software Group of the European Synchrotron Radiation Facility (ESRF) (PyMca). The data are reported in Tables S3–S8, respectively, and examples of curve fitting are given in Fig. S5. From this procedure, the intensity ratios, defined as the ratio between the peak areas ascribed to K_α lines of two different elements, were calculated. For the powdered samples, a mean value with the corresponding standard deviation is calculated for each Monte Arci sub-source (intra-source variance on powders). The data on the intact samples are reported as mean values with the corresponding standard deviations for three independent measurements (intra-sample variance, see **paragraph 2.1**).

2.5. Multivariate analysis

The data were also analysed by means of multivariate analysis through the R-based software CAT (Chemometric Agile Tool) (R. Leardi, C. Melzi, G. Polotti, CAT (Chemometric Agile Tool), freely downloadable from http://gruppochemiometria.it/index.php/software).

3. Results

3.1. Bi-/trivariate analysis of powdered geological obsidian samples

Once the experimental conditions were selected as 25 kV, 0.150 mA, 5 mm-beam shutter, 960 s, after an initial study described in the **paragraph S.1** of the Supporting Information, sixteen samples of known provenance (Table S2) were analysed in form of powders to inspect the potentiality of the available pXRF spectrophotometer in discriminating the Monte Arci obsidian sub-sources (Fig. 2). This first set of analysis runs permitted to evaluate the discriminating power of this tool on ideal, *i.e.*, homogenous, and planar samples, beyond those limits typical of intact objects in terms of chemical and morphological inhomogeneities (in particular concerning roughness and thickness). Potassium (K), calcium (Ca), titanium (Ti), manganese (Mn), iron (Fe), zinc (Zn), rubidium (Rb), and strontium (Sr) were visible as K_α and K_β lines in a typical XRF spectrum of obsidian. As expected, the K_β lines of some elements (K, Mn, Sr) overlapped with the K_α lines of others (Ca, Fe, Zr, respectively). Additional peaks associated with K_α and K_β lines of molybdenum (X-ray source, E (K_α) = 17.48 keV), K_α of argon (present in the 1 cm-air cushion between the sample and the analytical head of the instrument), and elastic/inelastic scattering phenomena above 16 keV were also visible (Fig. 2a). Light elements contributed by enhancing the background signal as Bremsstrahlung radiation.

Fig. 2b and c shows qualitatively differences on the XRF spectra of the different Monte Arci sub-sources (normalised with respect to Fe K_α intensity, which is the most intense peak): (i) Ti K_α intensity increases in the order SA < SB2 < SB1 < SC; (ii) Mn K_α intensity increases in the order SC < SB1 < SB2 < SA; (iii) Zn K_α intensity increases in the order SB2 < SC < SB1 < SA; (iv) Rb K_α intensity

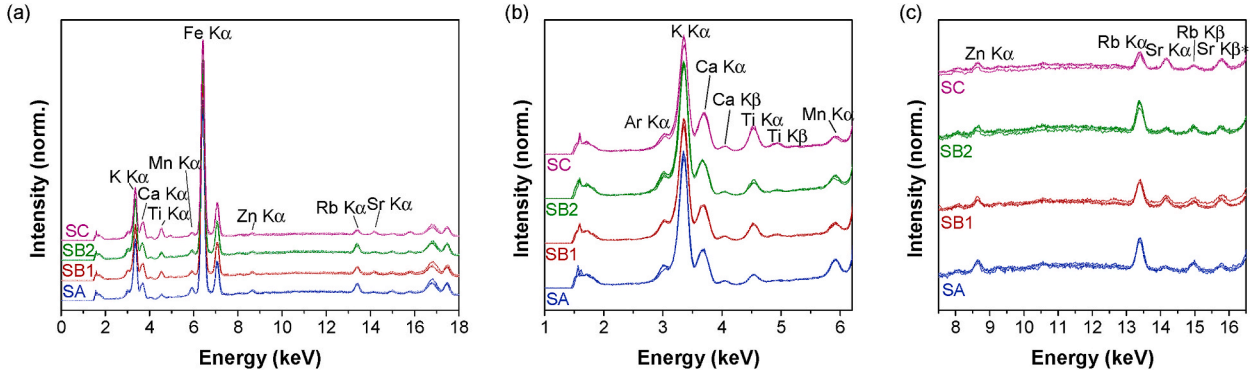

Fig. 2. XRF spectra of 16 obsidian samples analysed as powders, grouped on the basis of their provenance. *Sr K_β line is probably overlapped with Zr K_α line.

increases in the order SC < SB1 < SB2, SA; (v) Sr K_α intensity increases in the order SA < SB2 < SB1 < SC. Therefore, at least SA and SC groups seemed to be recognizable: SC features the highest intensities of Ti and Sr K_α lines, and the lowest for Mn and Rb ones, whereas the highest intensities of Mn and Zn K_α lines and the lowest for Ti and Sr ones seems to be typical of SA.

To extract semiquantitative discriminating criteria from XRF spectra of the powdered samples, a curve fitting was carried out by using three different software: LabLithos, Origin, PyMca (for further details see the **paragraph S.2** of the Supporting Information). The background was estimated in different ways depending on the software (Fig. S5). The data are listed in Tables S3–S6. LabLithos permitted to define the background thanks to the combination of values associated with smoothing, radius, and noise sensitivity. By Origin the background was profiled as an anchor point line by using 20 points. PyMca gave the possibility to choose between a peak stripping algorithm (STRIP) and a Statistical Nonlinear Iterative Peak clipping algorithm (SNIP). Here, two attempts were made by using two different backgrounds by which a different level of agreement between the experimental and calculated XRF spectra was obtained. Besides differences in the absolute values of relative areas, the trends in the mean values for the geochemical groups are the same regardless the adopted software (Fig. 3): (i) SA has the highest Rb/Fe, Zn/Fe and Mn/Fe, and the lowest Ti/Fe and Sr/Fe; (ii) SC has the highest Ti/Fe, Sr/Fe and the lowest Rb/Fe and Zn/Fe; (iii) SB1 has the same trend of SC but with higher (Rb/Fe, Zn/Fe) or lower (Ti/Fe, Sr/Fe) absolute values; (iv) SB2 has the same trend of SA but with higher (Ti/Fe, Sr/Fe) or lower (Rb/Fe, Zn/Fe) absolute values.

The comparison between the different softwares made us to prefer Origin and especially PyMca, and therefore, they were chosen for the next steps of the work (for further details see the **paragraph S.2** of the Supporting Information). These encouraging results led us to

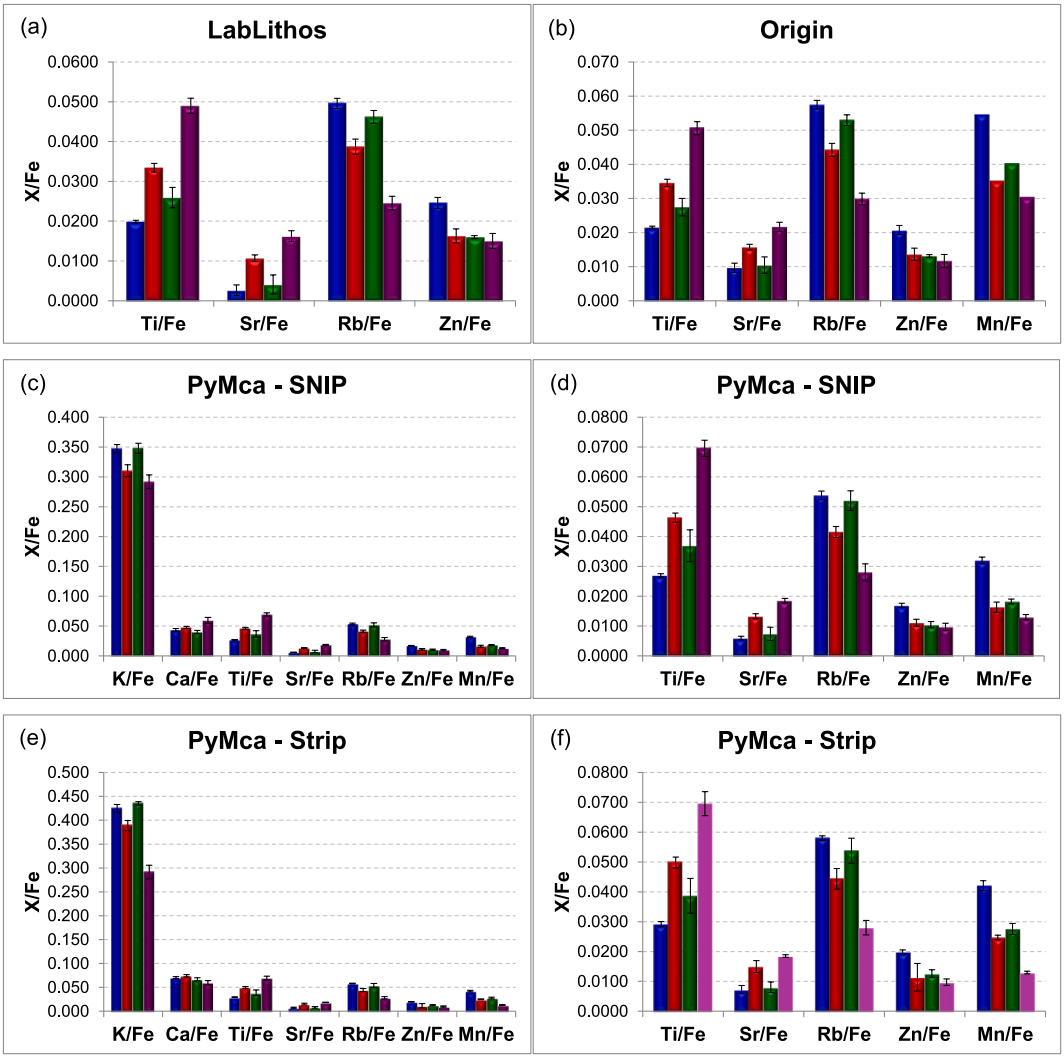

Fig. 3. Intensity ratios obtained from the XRF spectra of 16 powdered samples coming from the Monte Arci sub-sources (SA in blue, SB1 in red wine, SB2 in olive, SC in purple). The data were obtained by curve fitting with different software: LabLithos (a); Origin (b); PyMca by using a SNIP algorithm for the baseline (c, d); PyMca by using a Strip algorithm for the baseline (e, f). (For interpretation of the references to colour in this figure legend, the reader is referred to the Web version of this article.)

analyse also the intact geological samples, and among them those of unknown (for the chemists) provenance (blind test) to verify if a sub-source could be identified.

3.2. Bi-/trivariate analysis of intact geological samples

43 intact samples were analysed by pXRF and the data treated by Origin and PyMca software to obtain the intensity ratios with respect to the Fe K_α and to the Rb K_α. 38 samples were analysed in a blind test (Table S8), while 5 samples of known provenance (N426, N224, N225, N141, and N408, Table S7), also analysed as powders, were used to assign the groups to the geological sources. Three XRF spectra were collected on each sample and the mean values of the intensity ratios were reported in 2D-3D graphs to verify if the samples tend to form discrete groups according to different chemical composition. In the 2D graphs, the mean values are given with their standard deviation. In Fig. 4, the results obtained by Origin are presented. From the 2D plots, it is possible to distinguish 3 groups corresponding to SA, SB and SC. In particular, Ti/Fe *vs.* Mn/Fe and Ti/Fe *vs.* Zn/Fe allowed the distinction of the SA sub-source (Fig. 4a–d), while the SC group feature higher values of Ti/Rb, Sr/Rb, and Mn/Rb ratios (Fig. 4e–h). The sub-discrimination of the SB groups was also attempted by 3D plots, as those reported in Fig. 5, which makes clearer the discrimination of SC thanks to the higher values of Fe/Rb, Ti/Rb, and Sr/Rb ratios, while for SA groups the effect of lower Ti/Rb and Sr/Rb and higher Mn/Rb allows the SA samples to separately group at the bottom of the graph.

Based on this bi-/trivariate analysis a provenance assignment for the 38 intact and unknown geological samples was hypothesised, and compared with the actual provenance of the samples, as summarised in Table S9. All the samples were correctly recognised for their SA, SB and SC provenance, while three samples, were wrongly assigned (N509, N511) or not further distinguished (N515) for their SB1-SB2 provenance, leading to an error of the 8% in the assignment of SB samples (3/38 samples, or 3/18 SB samples leading to a 17%). In particular, if the sample N515 is at the edge of the hypothesised SB1-SB2 regions, the samples N509 and N511 appear to be more similar to the SB1 group members. The reason behind this behaviour was not associated with morphological issues in terms of thickness or flatness in these specific samples (Fig. S6). Therefore, in order to verify if these findings were a hint of a higher intra-source variance of the SB2 group, additional SA (+6 samples), SB1 (+5), SB2 (+13), SC (+1) samples were analysed. This latter SC sample (N238) was considered as an SB2 member based on its visual characters (visual characterization performed by C. Lugliè), but it was sourced in a secondary deposit in an area of possible SB2-SC mixing. Previous analysis by NAA ascribed an SC provenance to it, instead of an SB2 one. The data were fitted through the PyMca-SNIP approach, being the most promising one in terms of efficacy and timing. The SA members can be quite easily identified based on both 2D (Fig. 6) and 3D graphs (Fig. 7). All the SC samples can be recognised (even the sample N238 assigned as SB2 by visual characters but as SC by NAA), as well as the SB members. Therefore, a correct assignment was obtained with a 100% of success for the main SA, SB, and SC geochemical groups. On the contrary, the further distinction of the SB subgroups seems to be challenging due to a higher intra-source variability than previously hypothesised. In particular, some SB2 samples (N509, N511, N515, N232, N233, N353, N354, N355) and one SB1 obsidian (N230) are not assignable to an SB sub-source due to their distances in the 2D and 3D graphs from the other analogues. This led to a13% of error in the assignment. These results suggest a higher intra-source variability of the chemical composition of the SB2 samples, and the necessity of further

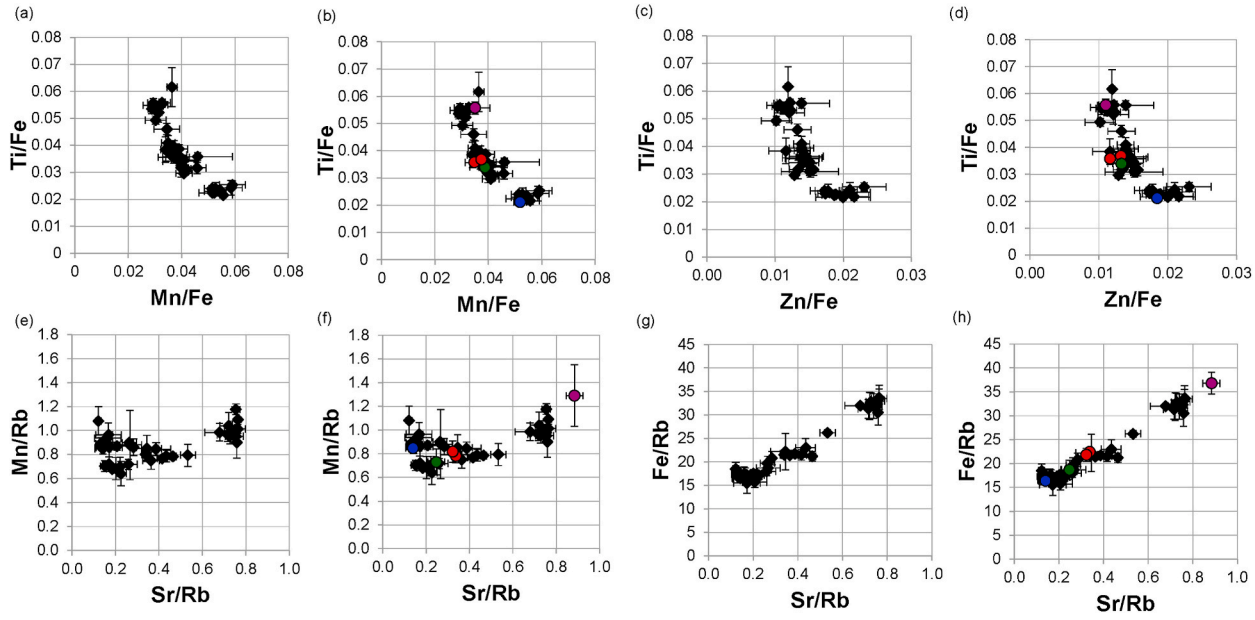

Fig. 4. 2D plots of different intensity ratios obtained by Origin for 43 intact obsidian samples coming from the Monte Arci sub-sources (blind test samples in black, SA in blue, SB1 in red wine, SB2 in olive, SC in purple): Ti/Fe *vs.* Mn/Fe (a, b); Ti/Fe *vs.* Zn/Fe (c, d); Mn/Rb *vs.* Sr/Rb (e, f); Fe/Rb *vs.* Sr/Rb (g, h). (For interpretation of the references to colour in this figure legend, the reader is referred to the Web version of this article.)

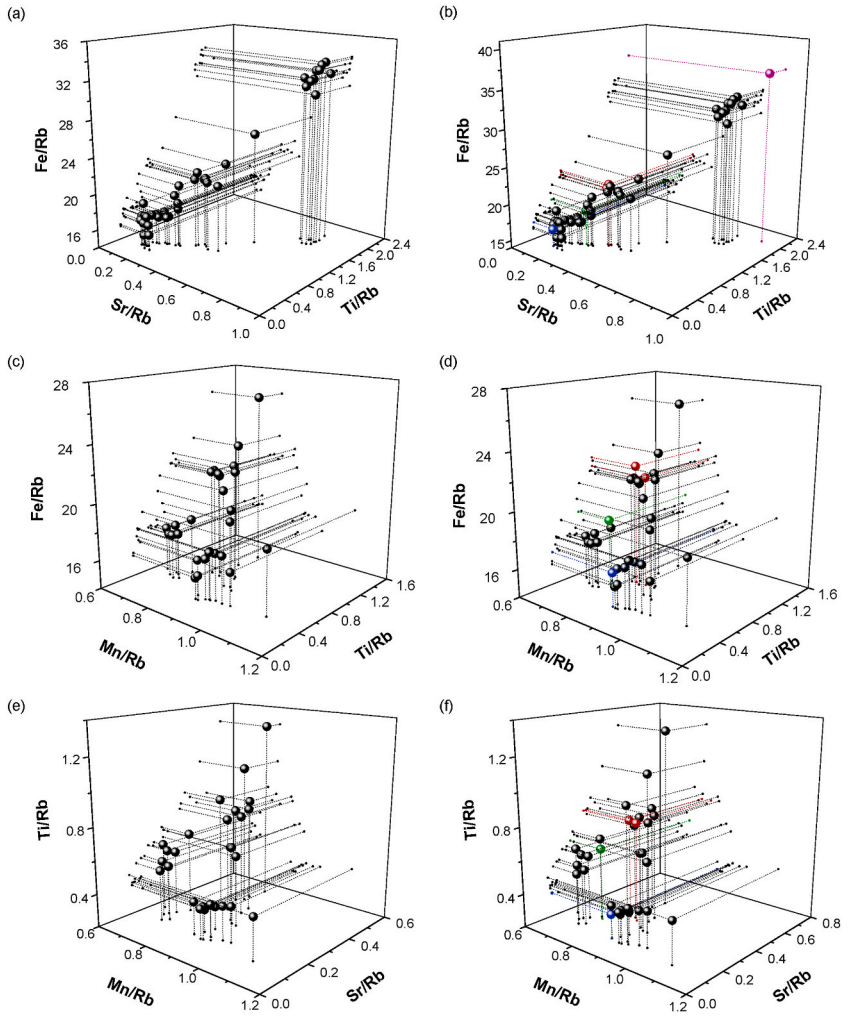

Fig. 5. 3D plots of different intensity ratios obtained by Origin for 43 intact obsidian samples coming from the Monte Arci sub-sources (blind test samples in black, SA in blue, SB1 in red wine, SB2 in olive, SC in purple): Fe/Rb *vs*. Ti/Rb *vs*. Sr/Rb (a, b); Fe/Rb *vs*. Ti/Rb *vs*. Mn/Rb (c, d); Ti/Rb *vs*. Sr/Rb *vs*. Mn/Rb (e, f). (For interpretation of the references to colour in this figure legend, the reader is referred to the Web version of this article.)

analysing a higher number of samples from this study and others reported in the literature to construct a more robust provenance study tool.

3.3. Analysis of archaeological samples

14 archaeological samples were analysed again for a blind-test in order to verify the possibility to hypothesise the provenance of obsidian artifacts with the as-built standardless bi-/trivariate model, based on the intensity ratios among K_α lines (Fig. 6 - right side, Fig. 7 – bottom part). The assignments are listed in Table 1, in comparison with the assignment based on previous analyses by PIXE or the visual characterization performed by C. Lugliè, and that based on the multivariate approach later discussed in this study (paragraph **3.4**) [60,62]. As shown, the assignments based on the two analytical techniques (pXRF and PIXE) perfectly matched, whereas for some of the samples a mismatching was observed when the results obtained by pXRF were compared with those obtained by visual characterization, as for the artifacts 422-274, CAR03, CAR06.

The agreement in the assignments based on pXRF and PIXE analyses of the archaeological samples from Su Carroppu, in contrast with the visual characterization, highlights the importance of developing a fast analytical tool able to distinguish among the three main geochemical groups, especially when taphonomic alterations of macroscopic features may render the visual assignment challenging.

The samples from the Middle Neolithic (MN) 422 structure at Cuccuru is Arrius were previously analysed by visual characterization, and the two assignments matched for three samples. The disagreement observed for the provenance of the sample 422-274 is not surprising due to the previously mentioned issues in the visual characterization and needs to be further investigated by other analytical technique. In this framework, the complete lithic collection coming from Cuccuru is Arrius is under study in a more

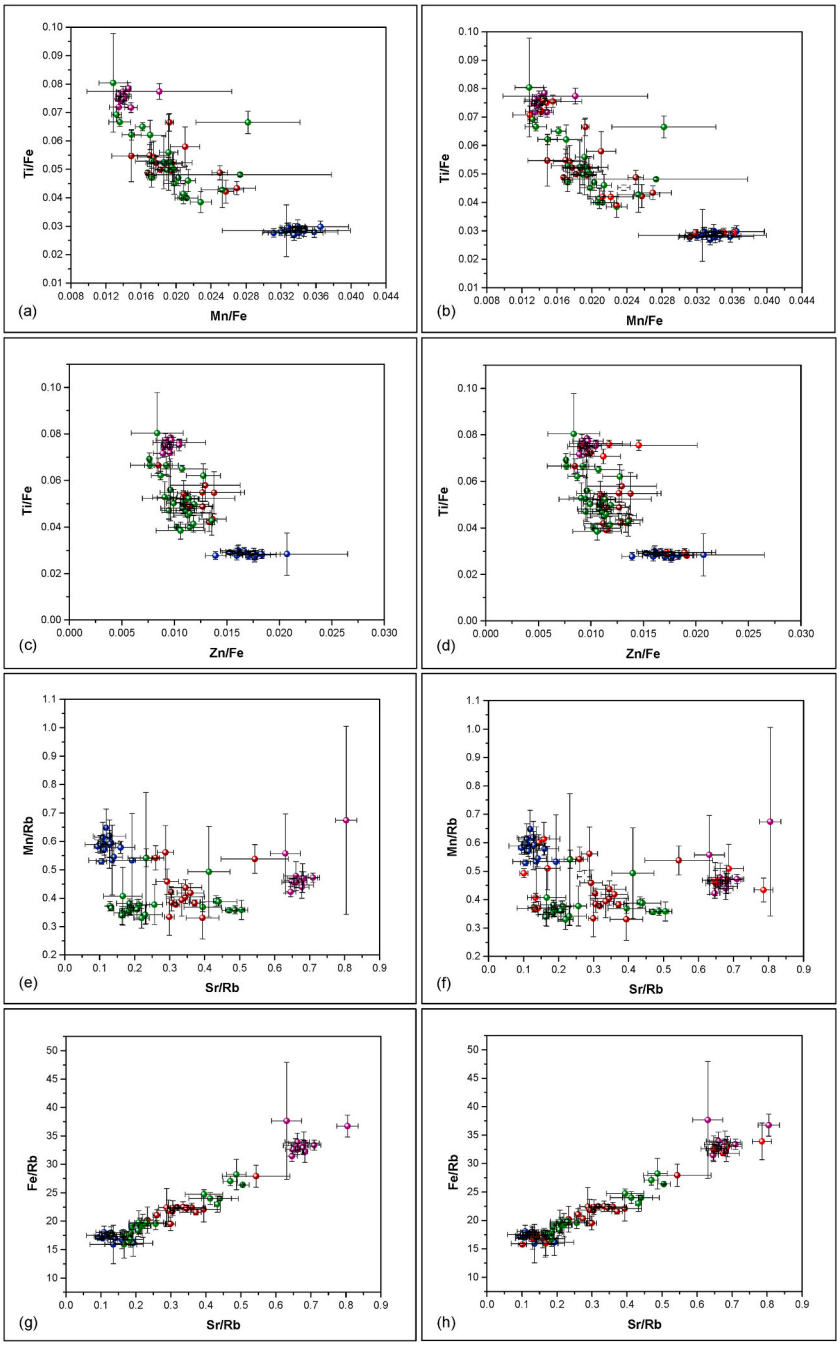

Fig. 6. 2D plots of different intensity ratios obtained by PyMca-SNIP for 68 intact obsidian samples coming from the Monte Arci sub-sources (SA in blue, SB1 in red wine, SB2 in olive, SC in purple): Ti/Fe *vs*. Mn/Fe (a, b); Ti/Fe *vs*. Zn/Fe (c, d); Mn/Rb *vs*. Sr/Rb (e, f); Fe/Rb *vs*. Sr/Rb (g, h). On the right, the same plots show the ratios for the 14 analysed artifacts (red spheres). (For interpretation of the references to colour in this figure legend, the reader is referred to the Web version of this article.)

comprehensive archaeometric research. Concerning the samples from Su Carroppu, the results show the following distribution in terms of provenance of the source: 50% from SC (5/10), 30% from SA (3/10), and only 2 artifacts came from SB groups, exclusively from SB2. These results need to be considered as preliminary, and we cannot conclude on the distribution of the raw matter in this site. Further analyses might be conducted on other obsidian artifacts found in Su Carroppu to investigate the archaeological aspects related to the use of obsidian.

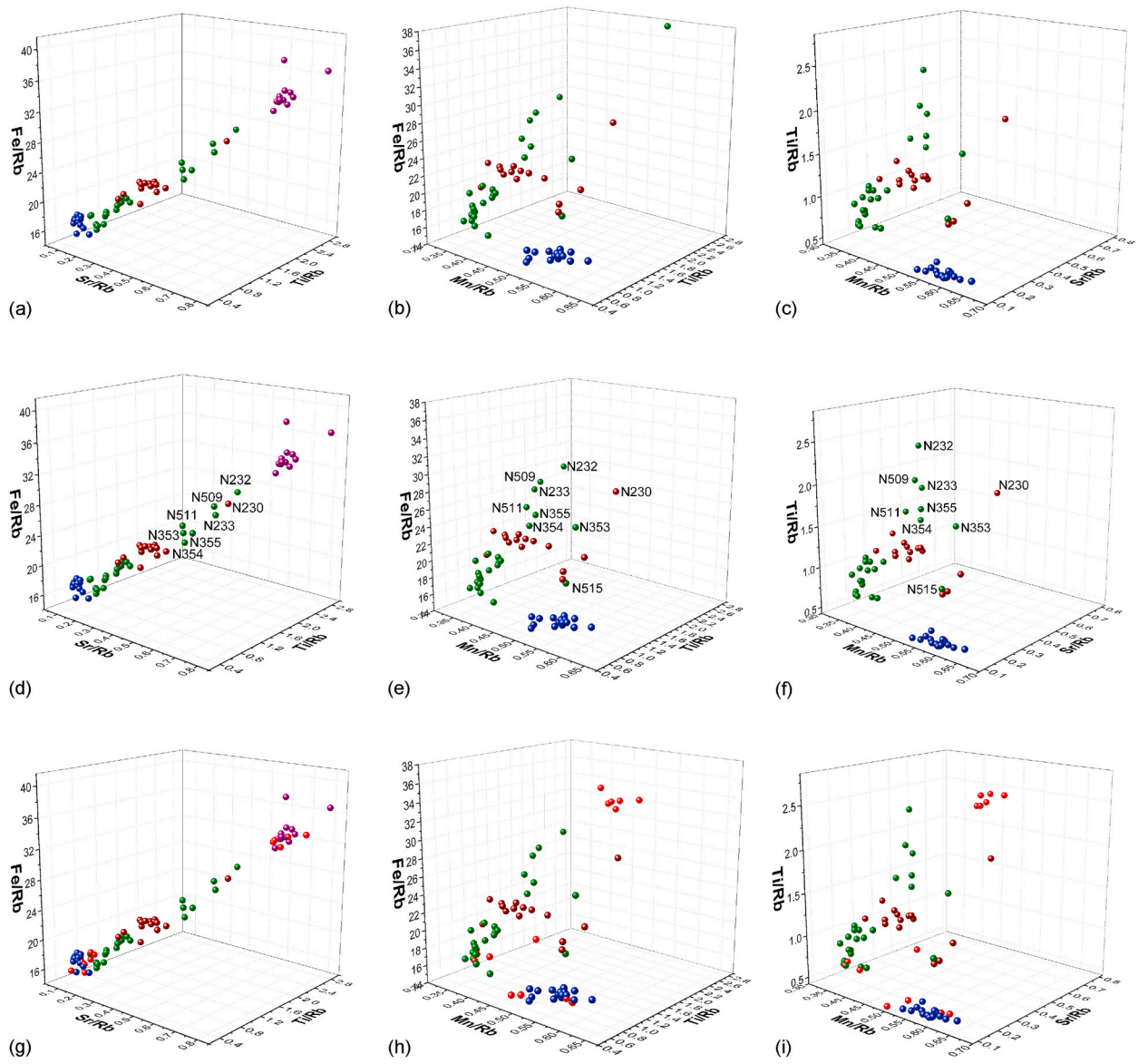

Fig. 7. 3D plots of different intensity ratios obtained by PyMCA-SNIP for 68 intact obsidian samples coming from the Monte Arci sub-sources (SA in blue, SB1 in red wine, SB2 in olive, SC in purple) (upper part). In the central part, the same graphs are provided with the labels to identify the samples that were wrongly assigned to the sub-sources. On the bottom part, the same plots are shown with the data for the 14 analysed artifacts (red spheres). From the left to the right: Fe/Rb *vs*. Ti/Rb *vs*. Sr/Rb (a, d, g); Fe/Rb *vs*. Ti/Rb *vs*. Mn/Rb (b, e, h); Ti/Rb *vs*. Sr/Rb *vs*. Mn/Rb (c, f, i). (For interpretation of the references to colour in this figure legend, the reader is referred to the Web version of this article.)

3.4. Multivariate analysis

An attempt to build an efficient method to identify the geochemical provenance of the obsidian samples was proposed based on multivariate analysis directly on the XRF spectra of the 68 geological intact samples. A schematic representation of the development steps of the multivariate method is shown in Fig. S7. The three XRF spectra acquired on each sample were averaged. Table 2 lists the four geochemical groups together with the number of samples, divided into training and test sets.

Within the whole spectral range, three main regions were selected: (1) region of the K_α and K_β lines of the Ti: from 4.2 keV to 5.2 keV, corresponding to the range in channels from 144 to 178; (2) region of the K_α and K_β lines of Mn, Fe, and Zn: from 5.5 keV to 10 keV, corresponding to the range in channels from 188 to 340; (3) region of lines K_α and K_β of Rb, Sr, and Zr: from 12.5 keV to 16.5 keV, corresponding to the range in channels from 425 to 559.

Fig. S8 shows the original XRF spectra, whereas the averaged spectra for the four different geological sub-sources are depicted in Fig. S9. The main differences already described for Fig. 2 are clearly visible: (i) the Zn and Mn peaks are more intense for the SA group;

Table 1
Provenance assignments of archaeological samples based on pXRF data treated by the bi-/trivariate and multivariate methods in comparison with those obtained from previous analyses by PIXE and visual characterization.

Sample	Assignment based on pXRF bi-/trivariate method (this study)	Assignment based on pXRF multivariate method (this study)	Assignment based on previous analyses	
			PIXE	Visual characterization
422–106	SB (SB1)	SB (SB2)	–	SB1
422–113	SA	SB (SB2)	–	SA
422–190	SC	SC	–	SC
422–274	SB (SB2)	SB (SB2)	–	SB1
CAR01	SC	SC	SC	SC
CAR02	SA	SA	SA	SA
CAR03	SB (SB2)	SB2	SB2	SA
CAR04	SC	SC	SC	SC
CAR05	SC	SC	SC	SC
CAR06	SB (SB2)	SB2	SB2	SA
CAR07	SA	SA	SA	SA
CAR08	SC	SC	SC	SC
CAR09	SA	SA	SA	SA
CAR10	SC	SC	SC	SC

Table 2
Number of samples from the four geochemical groups divided into training and test sets.

Geological origin	Training set	Test set
SA	12	5
SB1	10	5
SB2	18	7
SC	8	3
Tot	48	20

(ii) the Ti and Sr peaks are more intense for the SC group; (iii) SB groups have intermediate features between these two extremes, with SB1 more similar to SC, and SB2 to SA.

A supervised classification model was built by the chemometric tool of the k-nearest neighbours (*k-NN*), which is a distance-based discriminant method. It aims to classify test samples by the computation of their distances (multivariate Euclidean distances are commonly adopted) from all the samples in a training set of known class membership. The parameter *k*, which is the number of neighbours to be counted in the assignation rule, has to be defined and optimized within the training set. Then, the test sample is ascribed to that class with the majority representation in the *k* selected samples. If an odd *k* is selected, the *k-NN* delimiter is usually non-linear (depending on the number of *k*) and divides the space into as many subspaces as classes [94]. In this case, a probabilistic method such as the linear discriminant analysis (LDA) was not employed because the four classes (*i.e.*, the geochemical groups) feature a different variance-covariance matrix, being not characterized by the same dispersion and correlation structures [95].

Moreover, in order to obtain simple and more robust models, a genetic algorithm (GA) was applied, with the aim to select the informative regions of the spectra [96–98]

In the present work, a multi-step classification modelling was considered (Fig. S7). In the first step (Model A, Table 3), the model referred to the three main classes by making the SB1 and SB2 converge into the SB class (SA, SB, SC).

By applying the GA, the regions among the entire spectrum to better separate the three classes were chosen. Subsequently, a second model (Model B, Table 4) was built by considering separately the classes SB1 and SB2 (training set B = 28 samples). In this smaller training set, GA was applied again to select the spectral regions responsible for specific features useful to describe these two sub-classes.

All the samples predicted as SB in the first model were submitted to the second model as test set and it defined the actual geochemical membership between SB1 or SB2. Standard Normal Variate (SNV) and autoscaling were adopted as pre-treatments (Fig. S10). In both models the number of *k* for the *k*-NN algorithm was equal to 5. After the selection of the informative spectral

Table 3
Distribution of the spectra of the geological samples between the training and test set for the Model A, aimed to distinguish among the three main geochemical groups: SA, SB, SC.

Geological origin	Training set	Test set
SA	12	5
SB	28	11
SC	8	4
Tot	48	20

Table 4
Distribution of the spectra of the geological samples between the training and test set for the Model B, aimed to distinguish the SB subgroups: SB1, SB2.

Geological origin	Training set	Test set[a]
SB1	10	5
SB2	18	5
Tot	28	10

[a] Samples predicted as SB in the model A.

regions and before the computation of the classification models, a PCA was carried out on the training set as a data display method.

According to the GA results for Model A, 24 variables were selected. The energy (eV) intervals corresponding to the variables selected are shown in Fig. S11a and correspond to the Ti K_α (≈4.4–4.6 keV), Mn K_α (≈5.8–6.0 keV), Zn K_α (≈8.6 keV), and Rb K_α (≈13.3–13.5 keV). After the variable selection, the first PCA (Model A) was computed (Fig. 8), and two significant components explaining the 80.47% and 9.44% of the total variance (89.9%) were identified.

The score plot on the plane PC1-PC2 (Fig. 8), with the samples coloured according to the geochemical group, shows quite clearly that SA, SB and SC feature a specific location on the components plane, where SA and SC locate themselves at opposite scores on PC1 and at positive scores on PC2, while SB is at intermediate values on PC1 and at negative loadings on PC2. Only sample N232 (indicated in Fig. 8 as 39SB2) is confused with SC class. This sample appeared also problematic by bi-/trivariate analysis. SB category has the greatest variability with intermediate characteristics between SA and SC. Within SB, as expected, SB1 and SB2 appear to be confused with each other. For this reason, it has been chosen to reapply the GA to select specific features useful to better describe the two sub-classes. For classification purposes, as mentioned before, *k-NN* method was preferred on LDA due to the different dispersion and correlation structures of the classes.

By applying the GA on the samples predicted as SB from the Model A, 19 variables were selected. The energy (eV) intervals corresponding to the selected variables are shown in Fig. S11b. Together with the regions associated with the Zn K_α (≈8.7 keV) and Rb K_α (≈13.3–13.5 keV), the Sr Kα (≈14.1–14.2 keV) and a region between 9.5 and 9.6 keV were selected. This latter spectral region is associated with the baseline. The second PCA performed on samples predicted as SB by the first model (Model B) identifies 3 significant components explaining respectively 53.60%, 12.05%, and 8.30% of the total variance (73.95%) (Fig. 9, where only the first two components are shown).

The score plot on the plane PC1-PC2 (Fig. 9), with the samples coloured according to the geochemical membership, shows the two sub-classes quite separated along PC2, except for samples N356 (16SB2) and N230 (30SB1), respectively confused with SB1 and SB2 category. In particular, the sample N230 was not recognised as an SB1 member also by bi-/trivariate analysis. Furthermore, a greater variability is detected among the samples belonging to the SB2 class compared to those of the SB1 class, in agreement with the results obtained by bi-/trivariate analysis. The re-use of GA to select the informative region was necessary to better describe the two sub-classes and consequently to improve the classification rate.

Table 5 shows the confusion matrix in prediction with the corresponding correct predictions (%) for each class.

The geochemical group with the lowest percentage of correct prediction was SB2 (71%), whose samples were mainly confused with SC and SB1, while the others returned perfect predictions. The non-correctly assigned samples were 59SB2 (N509) and sample 65SB2 (N511), respectively predicted as SC and SB1, in agreement with the issues on these samples observed by bi-/trivariate analysis.

The as-built multivariate method, although it will need further improvement with the analysis of additional samples, was also applied to the archaeological samples, and the results are shown in Table 1. A correct assignment in agreement with bi-/trivariate pXRF and PIXE analyses, was obtained for 12 samples out of 14, with the 422-106 and 422-113 wrongly assigned to the SB2 subgroups,

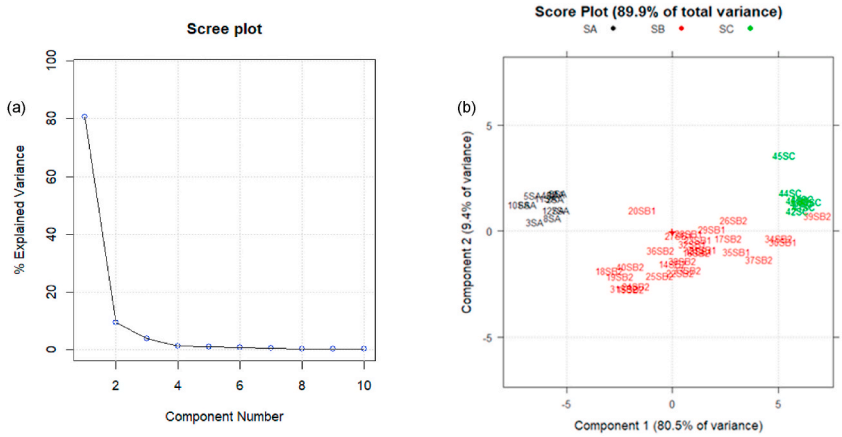

Fig. 8. Principal component analysis for the Model A: scree plot on the left (a), and score plot on the right (b).

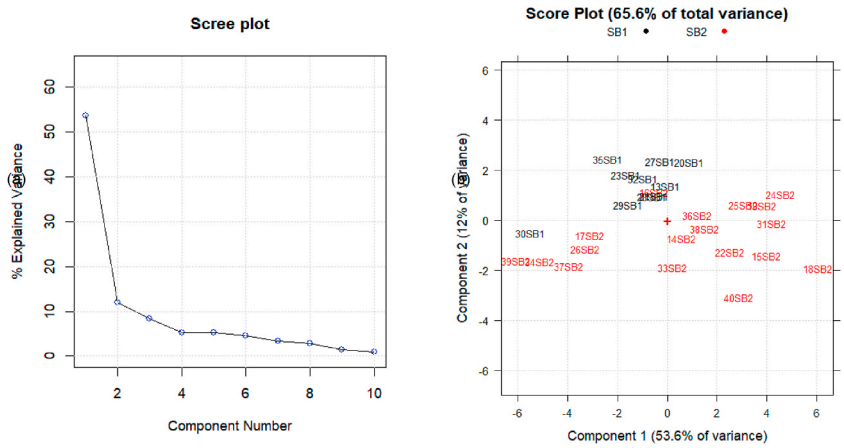

Fig. 9. Principal component analysis for the Model B: scree plot on the left (a), and score plot on the right (b).

Table 5
Confusion matrix in prediction with the corresponding percentage of correct predictions for each geochemical group.

Predicted geological origin	SA	SB1	SB2	SC	% Correct Predictions
SA	5	0	0	0	100
SB1	0	5	0	0	100
SB2	0	1	5	1	71
SC	0	0	0	4	100
% Total Correct Predictions					93

instead of SB1 and SA sources, respectively.

4. Discussion & conclusion

Nowadays, archaeological dissertations should be frequently based on archaeometry with analytical tools used not as black boxes but through a critical analysis of all possible sources of error. Once the archaeological objective has been defined, *e.g.*, in terms of provenance, function, technology questions, an analytical protocol based on the available instruments should be designed to build a non-destructive, time- and cost-effective routine.

As previously reported by other authors [74], pXRF spectroscopy has a lot of advantages in terms of easiness, low-cost, and speed of measurement, and depending on the available instrument allows the *in-situ* analysis in a non-destructive manner of differently sized-objects. In addition, this technique can be favourably used to determine the presence of high-atomic number elements, since the probability for an atom to relax from an excited state (reached as a consequence of the absorption of primary X-photons) through the physical phenomenon of fluorescence depends on the atomic number. Fortunately, for provenance purposes often the discriminative elements are heavy atoms easily detectable by this technique although present as few tens or hundreds of part per million [75]. The main obstacle in the wide use of this technique is related to the occurrence of the so-called "matrix effects", which makes it as a semi-quantitative method, unless the use of calibration and reference materials with similar matrix. Some issues might arise from the morphology of the analysed object in terms of thickness, roughness, and flatness, or weathering phenomena. Indeed, for a specific element, the intensity of the emission lines is not directly proportional to the concentration, and is affected by the presence of the other elements, *i.e.* the matrix. In particular, beside the concentration, the intensity is influenced by absorption, granulometric and surface effects [78]. In order to make these factors negligible, we have adopted the following solutions:

- although obsidian is a composite materials [37], the size of the analysed area was chosen big enough to obtain good quality spectra in terms of signal/noise ratio and an averaged information in the plane, making negligible the presence of microliths;
- the repeated analyses on three different areas of the same sample featuring different geometry permitted to obtain mean information, despite the differences in terms of surface effects, with a standard deviation accounting for the intra-sample variability;
- the construction of a database made on many intact geological samples (68 samples), not *a priori* selected on the basis of thickness, flatness, and roughness, allowed the occurrence of all the possible limits in terms of morphology detectable in the artifacts;
- the construction of a database where all the Monte Arci sub-sources are represented with at least ten samples, and where those problematic groups as SB2 have been over-represented to better evaluate the intra-source variability (17 from SA, 15 from SB1, 24 from SB2, 12 from SC);

- the adoption of a standardless method based on discriminative intensity ratios rather than absolute concentrations permits to skip the issues related to the quantification, taking into account that the X-rays emitted from two different elements in the same sample will be affected by the same matrix effects, and makes the method universal and independent on the specific pXRF instrument [78].

The results show the possibility to distinguish the main groups SA, SB, and SC. In particular, all the SA and SC samples are identified by the bi-/trivariate method, while a higher variability was detected for the SB1 and SB2 samples. The measurements performed, despite spanning over ten years, can be directly compared with a perfect match of the discriminative parameters, as observed for the SA samples, since the intensity ratios are not affected by changes in the absolute number of photons in the primary beam, *i.e.* aging of the X-ray tube over time.

In addition, a multivariate approach was attempted directly on the spectra with the aim of building a method independent on the analytical steps of data treatment, where from continuous variables, *i.e.*, the spectra, discrete variables are extracted, *i.e.* absolute concentrations or intensity ratios. Although different softwares (LabLithos, Origin, PyMca) led to similar discrimination powers among the Monte Arci sub-sources, the curve fitting procedure is the most time-consuming step in the process. Multivariate methods are commonly employed for provenance studies on obsidian based on discrete variables (absolute concentrations or intensity ratios) [52,53,63,68,74,80,99–111]. The direct application of multivariate analysis to XRF spectra was proposed in the literature for provenance studies on obsidian samples only in one case, associated with the study of Mesoamerican obsidian sources [112].

As indicated in the introduction, provenance studies on obsidian from Monte Arci dated back to the '60s, and some of them focused on the specific discrimination of Sardinian sub-sources [40,47,70,72–74,76–78,81]. A direct comparison with the literature is not so trivial, due to differences in the number of geological samples analysed by XRF, the adoption of multitechnique determination of the discriminative parameters, the focus on archaeological samples more than the description of the details in the analytical methods. For instance, percentage of errors in the determination of the provenance of the geological samples are often missing, probably due to the fact that the analytical method was not built in a "blind test" mode, as we did. The error bar in the bivariate plots is also not reported and sometimes samples at the edge of two different sub-sources regions are found. Surely, better discrimination might arise from the determination of other elements, such as Y, Nb, La, Ba, Zr, and Ga (Table S1), that were not visible in the XRF spectra acquired by the instrument here adopted. Nevertheless, we succeeded in developing a standardless method that might be similarly built on other instrument by other researchers and for other materials, once a large geological dataset is available and the sources appear different for elements detectable with that instrument, but without the necessity of quantitative parameters. Despite local impacts, this work might be useful for researchers dealing with provenance studies to develop standardless methods by the available pXRF, on other obsidian sources, and even other materials archaeologically relevant. The preliminary results here presented are promising with a 100% of SA, SB1 and SC samples correctly predicted but a 71% of success in the case of SB2 geological members. However, both the methodologies agree in suggesting the limits in identifying the obsidian samples from SB2, associated with a higher compositional variability, and defines the necessity to further enlarge the analysed samples to build even more robust classification methods. The analyses on 14 artifacts revealed the agreement of classification between the approaches here and previous analyses by PIXE on ten samples (CAR01-CAR10).

Author contribution statement

Valentina Mameli: Conceived and designed the experiments; Performed the experiments; Analyzed and interpreted the data; Wrote the paper.

Marco Sanna Angotzi: Performed the experiments; Analyzed and interpreted the data; Wrote the paper.

Emanuele Farinini, Riccardo Leardi: Analyzed and interpreted the data; Wrote the paper.

Carlo Lugliè: Analyzed and interpreted the data; Contributed reagents, materials, analysis tools or data; Wrote the paper.

Carla Cannas: Conceived and designed the experiments; Analyzed and interpreted the data; Contributed reagents, materials, analysis tools or data; Wrote the paper.

Funding statement

Dr. Valentina Mameli was supported by PON AIM (PON Ricerca e Innovazione 2014–2020–Azione I.2–DD n. 407 del 27 febbraio 2018 "Attraction and International Mobility", CultGeoChim project [AIM1890410-3].

Data availability statement

Data included in article/supp. material/referenced in article.

Declaration of interest's statement

The authors declare no competing interests.

Acknowledgements

Prof. François-Xavier Le Bourdonnec, from Université Bordeaux Montaigne, Archéosciences Bordeaux UMR 6034 is really

acknowledged for PIXE analyses.

Appendix A. Supplementary data

Supplementary data to this article can be found online at https://doi.org/10.1016/j.heliyon.2023.e13958.

References

[1] A.M. Pollard, C. Heron, Archaeological Chemistry, Royal Society of Chemistry, Cambridge, 1996, https://doi.org/10.1039/9781847550156.
[2] J.E. Ericson, A. Makishima, J.D. Mackenzie, R. Berger, Chemical and physical properties of obsidian: a naturally occurring glass, J. Non-Cryst. Solids 17 (1975) 129–142, https://doi.org/10.1016/0022-3093(75)90120-9.
[3] G. Longworth, S.E. Warren, The application of Mössbauer spectroscopy to the characterisation of western mediterranean obsidian, J. Archaeol. Sci. 6 (1979) 179–193, https://doi.org/10.1016/0305-4403(79)90061-X.
[4] F. Chavez-Rivas, J.R. Régnard, J. Chappert, Mössbauer study of natural glasses : lipari and teotihuacan obsidians, J. Phys. Colloq. 41 (1980) C1–C275, https://doi.org/10.1051/jphyscol:1980196. C1-276.
[5] F. Aramu, V. Maxia, S. Serci, I. Uras, Mössbauer study of mount Arci (Sardinia) obsidian, Lett. Al Nuovo Cim. Ser. 2 36 (1983) 102–104, https://doi.org/10.1007/BF02749650.
[6] B. Spiering, F.A. Seifert, Iron in silicate glasses of granitic composition: a Mössbauer spectroscopic study, Contrib. Mineral. Petrol. 90 (1985) 63–73, https://doi.org/10.1007/BF00373042.
[7] E. Schmidbauer, E. Mosheim, N. Semioschkina, Magnetization and 57Fe Mössbauer study of obsidians, Phys. Chem. Miner. 13 (1986) 256–261, https://doi.org/10.1007/BF00308277.
[8] F. Chávez-Rivas, R. Zamorano-Ulloa, D. Galland, J.R. Regnard, J. Chappert, Ferro and paramagnetic resonance studies of natural volcanic glasses: teotihuacan obsidians, J. Appl. Phys. 70 (1991) 5849–5851, https://doi.org/10.1063/1.350133.
[9] M. Okuno, H. Iwatsuki, T. Matsumoto, Structural analysis of an obsidian by X-ray diffraction method, Eur. J. Mineral 8 (1996) 1257–1264, https://doi.org/10.1127/ejm/8/6/1257.
[10] T.G. Sharp, R.J. Stevenson, D.B. Dingwell, Microlites and “nanolites” in rhyolitic glass: microstructural and chemical characterization, Bull. Volcanol. 56 (1996) 631–640, https://doi.org/10.1007/s004450050116.
[11] D. Tenorio, P. Bosch, M. Jimenez Reyes, S. Bulbulian, Differences in coloured obsidians from Sierra de Pachuca, Mexico, J. Archaeol. Sci. 25 (1998) 229–234, https://doi.org/10.1006/jasc.1997.0236.
[12] P. Acquafredda, T. Andriani, S. Lorenzoni, E. Zanettin, Chemical characterization of obsidians from different mediterranean sources by non-destructive SEM-EDS analytical method, J. Archaeol. Sci. 26 (1999) 315–325, https://doi.org/10.1006/jasc.1998.0372.
[13] C. Ma, J. Gresh, G.R. Rossman, G.C. Ulmer, E.P. Vicenzi, Micro-analytical study of the optical properties of rainbow and sheen obsidians, Can. Mineral. 39 (2001) 57–71.
[14] R.B. Scorzelli, S. Petrick, A.M. Rossi, G. Poupeau, G. Bigazzi, Obsidian archaeological artefacts provenance studies in the Western Mediterranean basin: an approach by Mössbauer spectroscopy and electron paramagnetic resonance, Comptes Rendus l’Académie Des Sci. - Ser. IIA - Earth Planet. Sci. 332 (2001) 769–776, https://doi.org/10.1016/S1251-8050(01)01598-1.
[15] C.A. Vásquez, H.G. Nami, A.E. Rapalini, Magnetic sourcing of obsidians in southern south America: some successes and doubts, J. Archaeol. Sci. 28 (2001) 613–618, https://doi.org/10.1006/jasc.2000.0611.
[16] M. Duttine, G. Villeneuve, G. Poupeau, a.M. Rossi, R.B. Scorzelli, Electron spin resonance of Fe3+ ion in obsidians from Mediterranean islands. Application to provenance studies, J. Non-Cryst. Solids 323 (2003) 193–199, https://doi.org/10.1016/S0022-3093(03)00306-5.
[17] A. Milleville, L. Bellot-Gourlet, B. Champagnon, D. Santallier, La Micro-spectroscopie Raman pour l’étude des Obsidiennes: structure, Micro-inclusions et études de provenance? Rev. d’Archéométrie. 27 (2003) 123–130, https://doi.org/10.3406/arsci.2003.1048.
[18] S.J. Stewart, G. Cernicchiaro, R.B. Scorzelli, G. Poupeau, P. Acquafredda, A. De Francesco, Magnetic properties and 57Fe Mössbauer spectroscopy of Mediterranean prehistoric obsidians for provenance studies, J. Non-Cryst. Solids 323 (2003) 188–192, https://doi.org/10.1016/S0022-3093(03)00305-3.
[19] N. Zotov, Structure of natural volcanic glasses: diffraction versus spectroscopic perspective, J. Non-Cryst. Solids 323 (2003) 1–6, https://doi.org/10.1016/S0022-3093(03)00289-8.
[20] P. Acquafredda, A. Paglionico, SEM-EDS microanalysis of microphenocrysts of Mediterranean obsidians: a preliminary approach to source discrimination, Eur. J. Mineral 16 (2004) 419–429, https://doi.org/10.1127/0935-1221/2004/0016-0419.
[21] V. Kovács Kis, I. Dódony, J.L. Lábár, Amorphous and partly ordered structures in SiO2 rich volcanic glasses, An ED study, Eur. J. Mineral. 18 (2006) 745–752, https://doi.org/10.1127/0935-1221/2006/0018-0745.
[22] A. Bustamante, M. Delgado, R.M. Latini, A.V.B. Bellido, Multivariate analysis in provenance studies: cerrillos obsidians case, Peru, Hyperfine Interact. 175 (2007) 43–48, https://doi.org/10.1007/s10751-008-9586-z.
[23] C. Ma, G.R. Rossman, J.A. Miller, The origin of color in “fire” obsidian, Can. Mineral. 45 (2007) 551–557, https://doi.org/10.2113/gscanmin.45.3.551.
[24] V.S. Rusakov, M.V. Volovetskii, O.A. Lukanin, Mössbauer studies of natural glasses of impact and volcanic origin, Moscow Univ. Phys. Bull. 62 (2007) 187–192, https://doi.org/10.3103/S0027134907030149.
[25] P. Acquafredda, I.M. Muntoni, Obsidian from pulo di Molfetta (bari, southern Italy): provenance from lipari and first recognition of a neolithic sample from Monte Arci (Sardinia), J. Archaeol. Sci. 35 (2008) 947–955, https://doi.org/10.1016/j.jas.2007.06.017.
[26] M. Duttine, R.B. Scorzelli, G. Cernicchiaro, G. Poupeau, N. Guillaume-Gentil, Magnetic properties and electron spin resonance of Ecuadorian obsidians. Application to provenance research of archeological samples, J. Magn. Magn Mater. 320 (2008) 136–138, https://doi.org/10.1016/j.jmmm.2008.02.030.
[27] E.A. Carter, M.D. Hargreaves, N. Kononenko, I. Graham, H.G.M. Edwards, B. Swarbrick, R. Torrence, Raman spectroscopy applied to understanding prehistoric obsidian trade in the pacific region, Vib. Spectrosc. 50 (2009) 116–124, https://doi.org/10.1016/j.vibspec.2008.09.002.
[28] S.J. Kelloway, N. Kononenko, R. Torrence, E.A. Carter, Assessing the viability of portable Raman spectroscopy for determining the geological source of obsidian, Vib. Spectrosc. 53 (2010) 88–96, https://doi.org/10.1016/j.vibspec.2010.02.006.
[29] A. Ferk, R. Leonhardt, K.U. Hess, D.B. Dingwell, Paleointensities on 8 ka obsidian from mayor island, New Zealand, Solid Earth 2 (2011) 259–270, https://doi.org/10.5194/se-2-259-2011.
[30] A. Ferk, R. Leonhardt, F.W. Von Aulock, K.U. Hess, D.B. Dingwell, Paleointensities of phonolitic obsidian: influence of emplacement rotations and devitrification, J. Geophys. Res. Solid Earth 116 (2011) 1–18, https://doi.org/10.1029/2011JB008397.
[31] E. Cañón-Tapia, K. Cárdenas, Anisotropy of magnetic susceptibility and magnetic properties of obsidians: volcanic implications, Int. J. Earth Sci. 101 (2012) 649–670, https://doi.org/10.1007/s00531-011-0687-6.
[32] K. Tanaka, N. Nemoto, Photoluminescence of obsidian: a particle-dispersed natural glass, Phys. Status Solidi 9 (2012) 2308–2311, https://doi.org/10.1002/pssc.201200188.
[33] E. Zanella, E. Ferrara, L. Bagnasco, A. Ollà, R. Lanza, C. Beatrice, Magnetite grain-size analysis and sourcing of Mediterranean obsidians, J. Archaeol. Sci. 39 (2012) 1493–1498, https://doi.org/10.1016/j.jas.2011.12.030.

[34] E. Frahm, J.M. Feinberg, From flow to quarry: magnetic properties of obsidian and changing the scale of archaeological sourcing, J. Archaeol. Sci. 40 (2013) 3706–3721, https://doi.org/10.1016/j.jas.2013.04.029.

[35] L.E. Waters, R.A. Lange, Crystal-poor, multiply saturated rhyolites (obsidians) from the Cascade and Mexican arcs: evidence of degassing-induced crystallization of phenocrysts, Contrib. Mineral. Petrol. 166 (2013) 731–754, https://doi.org/10.1007/s00410-013-0919-9.

[36] E. Frahm, J.M. Feinberg, B.A. Schmidt-Magee, K. Wilkinson, B. Gasparyan, B. Yeritsyan, S. Karapetian, K. Meliksetian, M.J. Muth, D.S. Adler, Sourcing geochemically identical obsidian: multiscalar magnetic variations in the Gutansar volcanic complex and implications for Palaeolithic research in Armenia, J. Archaeol. Sci. 47 (2014) 164–178, https://doi.org/10.1016/j.jas.2014.04.015.

[37] V. Mameli, A. Musinu, D. Niznansky, D. Peddis, G. Ennas, A. Ardu, C. Lugliè, C. Cannas, Much more than a glass: the complex magnetic and microstructural properties of obsidian, J. Phys. Chem. C 120 (2016) 27635–27645, https://doi.org/10.1021/acs.jpcc.6b08387.

[38] C. Lugliè, L'obsidienne néolithique en Méditerranée occidentale, in: M.-H. Moncel, F. Fröhlich (Eds.), L'Homme Le Précieux. Matières Minérales Précieuses La Préhistoire à Aujourd'hui, British Ar, Archeopress, Oxford, 2009, pp. 213–224.

[39] C. Lugliè, From the perspective of the source. Neolithic production and exchange of Monte Arci obsidians (Central-Western Sardinia), in: Congrés Int. Xarxes Al Neolític – Neolit. Networks, 2012, pp. 173–180.

[40] R.H. Tykot, Chemical fingerprinting and source tracing of obsidian: the central mediterranean trade in black gold, Acc. Chem. Res. 35 (2002) 618–627, https://doi.org/10.1021/ar000208p.

[41] J. Zilhão, D.E. Angelucci, F.-X. Le Bourdonnec, A. Lucena, I. Martín-Lerma, S. Martínez, H. Matias, V. Villaverde, J. Zapata, Obsidian in the upper palaeolithic of iberia, Antiquity 95 (2021) 865–884, https://doi.org/10.15184/aqy.2021.85.

[42] G. Poupeau, F.-X. Le Bourdonnec, S. Dubernet, R.B. Scorzelli, M. Duttine, T. Carter, Tendances actuelles dans la caractérisation des obsidiennes pour les études de provenance, ArcheoSciences, Rev. d'Archéométrie. 31 (2007) 79–86. http://archeosciences.revues.org/772.

[43] P.C. Weigand, G. Harbottle, E.V. Sayre, Turquoise Sources and Source Analysis: Mesoamerica and the Southwestern U.S.A, in: Exch. Syst. Prehistory, Elsevier, 1977, pp. 15–34, https://doi.org/10.1016/B978-0-12-227650-7.50008-0.

[44] H. Neff, Neutron Activation Analysis for Provenance Determination in Archaeology, in: E. Ciliberto, G. Spoto (Eds.), Mod. Anal. Methods Art Archaeol., Wiley & Sons, 2000. http://eu.wiley.com/WileyCDA/WileyTitle/productCd-047129361X.html.

[45] M. Rapisarda, L'età dell'ossidiana di Pantelleria, AAPP Atti Della Accad. Peloritana Dei Pericolanti, Cl. Di Sci. Fis. Mat. e Nat. 85 (2007) 1–21, https://doi.org/10.1478/C1C0702001.

[46] J.R. Cann, C. Renfrew, The characterization of obsidian and its application to the Mediterranean Region, Prehist. Soc. 8 (1964) 111–133, https://doi.org/10.1017/S0079497X00015097.

[47] R.H. Tykot, Characterization of the Monte Arci (Sardinia) obsidian sources, J. Archaeol. Sci. 24 (1997) 467–479, https://doi.org/10.1006/jasc.1996.0130.

[48] C. Lugliè, F.X. Le Bourdonnec, G. Poupeau, M. Bohn, S. Meloni, M. Oddone, G. Tanda, A map of the Monte Arci (Sardinia Island, Western Mediterranean) obsidian primary to secondary sources. Implications for Neolithic provenance studies, Comptes Rendus Palevol 5 (2006) 995–1003, https://doi.org/10.1016/j.crpv.2006.09.007.

[49] O.W. Thorpe, S.E. Warren, J. Courtin, The distribution and sources of archaeological obsidian from southern France, J. Archaeol. Sci. 11 (1984) 135–146, https://doi.org/10.1016/0305-4403(84)90048-7.

[50] P. Avino, A. Rosada, Mediterranean and near east obsidian reference samples to establish artefacts provenance, Herit. Sci. 2 (2014) 1–11, https://doi.org/10.1186/s40494-014-0016-z.

[51] P. Avino, P. Moioli, A. Rosada, C. Seccaroni, Obsidian use in the mosaic of the St. Juvenal church, Narni (Italy): Chemical characterization and origin, Herit. Sci. 1 (2013) 1–8, https://doi.org/10.1186/2050-7445-1-17.

[52] C. Seccaroni, N. Volante, A. Rosada, L. Ambrosone, G. Bufalo, P. Avino, Identification of provenance of obsidian samples analyzing elemental composition by INAA, J. Radioanal. Nucl. Chem. 278 (2008) 277–282. https://link.springer.com/10.1007/s10967-008-0502-4.

[53] S. Meloni, C. Lugliè, M. Oddone, L. Giordani, Diffusion of obsidian in the Mediterranean basin in the neolithic period: A trace element characterization of obsidian from Sardinia by instrumental neutron activation analysis, J. Radioanal. Nucl. Chem. 271 (2007) 533–539, https://doi.org/10.1007/s10967-007-0302-2.

[54] A.J. Ammerman, A. Cesana, C. Polglase, M. Terrani, Neutron activation analysis of obsidian from two Neolithic sites in Italy, J. Archaeol. Sci. 17 (1990) 209–220, https://doi.org/10.1016/0305-4403(90)90060-I.

[55] F.X. Le Bourdonnec, G. Poupeau, F. Lorenzi, P. Machut, J. Sicurani, Typologie et provenance de l'obsidienne du site néolithique d'AGuaita (NW Cap Corse, Corse, France), Comptes Rendus Palevol 13 (2014) 317–331, https://doi.org/10.1016/j.crpv.2013.10.005.

[56] F.X. Le Bourdonnec, A. D'Anna, G. Poupeau, C. Lugliè, L. Bellot-Gurlet, P. Tramoni, H. Marchesi, Obsidians artefacts from Renaghju (Corsica Island) and the Early Neolithic circulation of obsidian in the Western Mediterranean, Archaeol. Anthropol. Sci. 7 (2015) 441–462, https://doi.org/10.1007/s12520-014-0206-3.

[57] F.X. Le Bourdonnec, G. Poupeau, C. Lugliè, A. D'Anna, L. Bellot-Gurlet, C.S. Bressy-Leandri, A. Pasquet, P. Tramoni, New data and provenance of obsidian blocks from Middle Neolithic contexts on Corsica (western Mediterranean), Comptes Rendus Palevol 10 (2011) 259–269, https://doi.org/10.1016/j.crpv.2011.01.001.

[58] C.S. Bressy, A. D'Anna, G. Poupeau, F.X. Le Bourdonnec, L. Bellot-Gurlet, F. Leandri, P. Tramoni, F. Demouche, Chert and obsidian procurement of three Corsican sites during the 6th and 5th millenniums BC, Comptes Rendus Palevol 7 (2008) 237–248, https://doi.org/10.1016/j.crpv.2008.02.007.

[59] F.X.L. Bourdonnec, S. Delerue, S. Dubernet, P. Moretto, T. Calligaro, J.C. Dran, G. Poupeau, PIXE characterization of Western Mediterranean and Anatolian obsidians and Neolithic provenance studies, Nucl. Instrum. Methods Phys. Res. Sect. B Beam Interact. Mater. Atoms 240 (2005) 595–599, https://doi.org/10.1016/j.nimb.2005.06.156.

[60] C. Lugliè, F.-X. Le Bourdonnec, G. Poupeau, E. Atzeni, S. Dubernet, P. Moretto, L. Serani, Early Neolithic obsidians in Sardinia (Western Mediterranean): the Su Carroppu case, J. Archaeol. Sci. 34 (2007) 428–439, https://doi.org/10.1016/j.jas.2006.06.002.

[61] G. Poupeau, L. Bellot-Gurlet, V. Brisotto, O. Dorighel, Nouvelles donnees sur la provenance de l'obsidienne des sites neolithiques du Sud-Est de la France, Comptes Rendus l'Academie Sci. - Ser. IIa Sci. La Terre Des Planetes. 330 (2000) 297–303, https://doi.org/10.1016/S1251-8050(00)00132-4.

[62] C. Lugliè, F.X. Le Bourdonnec, G. Poupeau, C. Congia, P. Moretto, T. Calligaro, I. Sanna, S. Dubernet, Obsidians in the Rio Saboccu (Sardinia, Italy) campsite: Provenance, reduction and relations with the wider Early Neolithic Tyrrhenian area, Comptes Rendus Palevol 7 (2008) 249–258, https://doi.org/10.1016/j.crpv.2007.11.001.

[63] F.X. Le Bourdonnec, J.M. Bontempi, N. Marini, S. Mazet, P.F. Neuville, G. Poupeau, J. Sicurani, SEM-EDS characterization of western Mediterranean obsidians and the Neolithic site of A Fuata (Corsica), J. Archaeol. Sci. 37 (2010) 92–106, https://doi.org/10.1016/j.jas.2009.09.016.

[64] D. Gimeno, Devitrification of natural rhyolitic obsidian glasses: Petrographic and microstructural study (SEM+EDS) of recent (Lipari island) and ancient (Sarrabus, SE Sardinia) samples, J. Non-Cryst. Solids 323 (2003) 84–90, https://doi.org/10.1016/S0022-3093(03)00294-1.

[65] F.X. Le Bourdonnec, G. Poupeau, C. Lugliè, SEM-EDS analysis of western Mediterranean obsidians: a new tool for Neolithic provenance studies, Compt. Rendus Geosci. 338 (2006) 1150–1157, https://doi.org/10.1016/j.crte.2006.09.018.

[66] P. Acquafredda, T. Andriani, S. Lorenzoni, E. Zanettin, Chemical Characterization of Obsidians from Di ff erent, J. Archaeol. Sci. 26 (1999) 315–325.

[67] A. Sciences, Petrography as a Method for Distinguishing, Cincinnati, Lloydia, 2000, pp. 43–58.

[68] Z. Kasztovszky, B. Maróti, I. Harsányi, D. Párkányi, V. Szilágyi, A comparative study of PGAA and portable XRF used for non-destructive provenancing archaeological obsidian, Quat. Int. 468 (2018) 179–189, https://doi.org/10.1016/j.quaint.2017.08.004.

[69] R.H. Tykot, Obsidian Studies in the Prehistoric Central Mediterranean: After 50 Years, What Have We Learned and What Still Needs to Be Done? Open Archaeol. 3 (2017) 264–278, https://doi.org/10.1515/opar-2017-0018.

[70] K.P. Freund, Lunati and the island of towers: Obsidian in Nuragic Sardinia, J. Archaeol. Sci. Reports. 21 (2018) 1–9, https://doi.org/10.1016/j.jasrep.2018.06.032.

[71] P.Y. Nicod, T. Perrin, F.X. Le Bourdonnec, S. Philibert, C. Oberlin, M. Besse, First Obsidian in the Northern French Alps during the Early Neolithic, J. Field Archaeol. 44 (2019) 180–194, https://doi.org/10.1080/00934690.2019.1580077.

[72] K.P. Freund, Contextualizing Bronze Age Obsidian Use at the 'Ritual Spring' of Mitza Pidighi (Sardinia), Sci. Technol. Archaeol. Res. 1 (2015) 1–10, https://doi.org/10.1080/20548923.2015.1110420.

[73] X. Terradas, B. Gratuze, J. Bosch, R. Enrich, X. Esteve, F.X. Oms, G. Ribé, Neolithic diffusion of obsidian in the Western Mediterranean: New data from Iberia, J. Archaeol. Sci. 41 (2014) 69–78, https://doi.org/10.1016/j.jas.2013.07.023.

[74] M. Orange, F.X. Le Bourdonnec, L. Bellot-Gurlet, C. Lugliè, S. Dubernet, C. Bressy-Leandri, A. Scheffers, R. Joannes-Boyau, On sourcing obsidian assemblages from the Mediterranean area: analytical strategies for their exhaustive geochemical characterisation, J. Archaeol. Sci. Reports. 12 (2017) 834–844, https://doi.org/10.1016/j.jasrep.2016.06.002.

[75] V. Francaviglia, Characterization of Mediterranean Obsidian Sources by Classical Petrochemical Methods, Preistoria Alp. 20 (1984) 311–332.

[76] K.P. Freund, R.H. Tykot, Lithic technology and obsidian exchange networks in Bronze Age Nuragic Sardinia (Italy), Archaeol. Anthropol. Sci. 3 (2011) 151–164, https://doi.org/10.1007/s12520-010-0047-7.

[77] K.P. Freund, Obsidian consumption in Chalcolithic Sardinia: A view from Bingia 'e Monti, J. Archaeol. Sci. 41 (2014) 242–250, https://doi.org/10.1016/j.jas.2013.08.016.

[78] A.M. De Francesco, G.M. Crisci, M. Bocci, Non-destructive analytic method using xrf for determination of provenance of archaeological obsidians from the mediterranean area: A comparison with traditional xrf methods, Archaeometry 50 (2008) 337–350, https://doi.org/10.1111/j.1475-4754.2007.00355.x.

[79] P. Acquafredda, I.M. Muntoni, M. Pallara, Reassessment of WD-XRF method for obsidian provenance shareable databases, Quat. Int. 468 (2018) 169–178, https://doi.org/10.1016/j.quaint.2017.08.020.

[80] A. Leck, F.X. Le Bourdonnec, B. Gratuze, S. Dubernet, N. Ameziane-Federzoni, C. Bressy-Leandri, R. Chapoulie, S. Mazet, J.M. Bontempi, N. Marini, M. Remicourt, T. Perrin, Provenance studies of Corsican rhyolite artefacts: Assessment of geochemical analysis methods, Comptes Rendus Palevol 17 (2018) 220–232, https://doi.org/10.1016/j.crpv.2017.10.003.

[81] C. Lugliè, F.X. Le Bourdonnec, G. Poupeau, Caratterizzazione elementare e provenienza delle ossidiane mediante analisi non distruttiva PIXE e EDXRF, in: M. Venturino Gambari (Ed.), La Mem. Del Passato. Castello Di Annone Tra Archeol. e Storia., LineLab ed, Alessandria, 2014, pp. 333–336.

[82] R. Tykot, Sourcing of Sardinian obsidian collections in the Museo Preistorico-Etnografico "Luigi Pigorini" using non-destructive portable XRF, L'ossidiana Del Monte Arci Nel Mediterr. Nuovi Apporti Sulla Diffus. Sui Sist. Di Prod. e Sulla Loro Cronologia, Atti Del 5° Convegno Internazionale (Pau, Ital. 27-29 Giugno 2008), a Cura Di C. Lugliè. NUR, Ales (2010) 27–29, 2010, http://shell.cas.usf.edu/~rtykot/PR80. Tykot 2010 - Pigorini obsidian.pdf.

[83] R.H. Tykot, L. Lai, C. Tozzi, Proceedings of the 37th International Symposium on Archaeometry, 13th - 16th May 2008, Siena, Italy, Springer Berlin Heidelberg, Berlin, Heidelberg, 2011, https://doi.org/10.1007/978-3-642-14678-7.

[84] R.H. Tykot, Using Nondestructive Portable X-ray Fluorescence Spectrometers on Stone, Ceramics, Metals, and Other Materials in Museums: Advantages and Limitations, Appl. Spectrosc. 70 (2016) 42–56, https://doi.org/10.1177/0003702815616745.

[85] R.H. Tykot, A Decade of Portable (Hand-Held) X-Ray Fluorescence Spectrometer Analysis of Obsidian in the Mediterranean: Many Advantages and Few Limitations, MRS Adv 2 (2017) 1769–1784, https://doi.org/10.1557/adv.2017.148.

[86] R.H. Tykot, Non-Destructive pXRF on Prehistoric Obsidian Artifacts from the Central Mediterranean, Appl. Sci. 11 (2021) 7459, https://doi.org/10.3390/app11167459.

[87] R.H. Tykot, Obsidian in Prehistory, in: Encycl. Glas. Sci. Technol. Hist. Cult., Wiley, 2021, pp. 1237–1248, https://doi.org/10.1002/9781118801017.ch10.1.

[88] M. La Monica, S. Rotolo, F. Foresta Martin, Petrographic and spectroscopic (FT-IR) study of Western Mediterranean obsidians geological sources and of a lithic collection from Ustica Island (Sicily), Ann. Geophys. Geophys. 61 (2019) 1–19, https://doi.org/10.4401/ag-8058.

[89] E. Ferrara, E. Tema, E. Zanella, C. Beatrice, F. Miola, E. Pavesio, A. Perino, Investigating the provenance of Italian archaeological obsidian tools based on their magnetic properties, Archaeol. Anthropol. Sci. 11 (2019) 3329–3341, https://doi.org/10.1007/s12520-018-0757-9.

[90] G. Poupeau, F.-X. Le Bourdonnec, M. Duttine, G. Villeneuve, S. Dubernet, C. Luglie, P. Moretto, L. Bellot-Gurlet, F. Frohlich, R.B. Scorzelli, I. Souza Azevedo, A. Lopez, S.J. Stewart, The Monte Arci Obsidian: New Fingerprinting Approaches in Provenance Studies, 2nd Convegno Internazional - L'ossidiana Del Monte Arci Nel Mediterr, 2004 ([PDF]).

[91] O. Bignon, N. Serrand, L.J. Costa, C. Lugliè, Les restes culinaires de Cuccuru is Arrius (Oristano, Sardaigne) : nouveaux apports à la connaissance des économies néolithiques en domaine littoral, Bull. La Société Préhistorique Française. 105 (2008) 773–785, https://doi.org/10.3406/bspf.2008.13784.

[92] M. Serra, V. Mameli, C. Cannas, Eneolithic menhirs of Laconi (central Sardinia, Italy): From provenance to technological properties, J. Archaeol. Sci. Reports. 5 (2016) 197–208, https://doi.org/10.1016/j.jasrep.2015.11.018.

[93] M. Serra, V. Mameli, C. Cannas, Geo-material provenance and technological properties investigation in Copper Age menhirs production at Allai (central-western Sardinia, Italy), STAR Sci. Technol. Archaeol. Res. 3 (2017) 391–404, https://doi.org/10.1080/20548923.2017.1417781.

[94] P. Oliveri, C. Malegori, M. Casale, Multivariate Classification Techniques, in: Ref. Modul. Chem. Mol. Sci. Chem. Eng., Elsevier, 2018, https://doi.org/10.1016/B978-0-12-409547-2.14239-8.

[95] P. Oliveri, C. Malegori, E. Mustorgi, M. Casale, Qualitative pattern recognition in chemistry: Theoretical background and practical guidelines, Microchem. J. 162 (2021), 105725, https://doi.org/10.1016/j.microc.2020.105725.

[96] D. Jouan-Rimbaud, D.L. Massart, O.E. de Noord, Random correlation in variable selection for multivariate calibration with a genetic algorithm, Chemometr. Intell. Lab. Syst. 35 (1996) 213–220, https://doi.org/10.1016/S0169-7439(96)00062-7.

[97] R. Leardi, Genetic Algorithms in Feature Selection, in: Genet. Algorithms Mol. Model., Elsevier, 1996, pp. 67–86, https://doi.org/10.1016/B978-012213810-2/50004-9.

[98] R. Leardi, Genetic algorithm-PLS as a tool for wavelength selection in spectral data sets, in: R. Leardi (Ed.), Nature-Inspired Methods Chemom. Genet. Algorithms Artif. Neural Networks, Data Handl., Sci. Technol. Ser., vol. 23, Elsevier, Amsterdam, 2003, pp. 169–196.

[99] D.J. Riebe, Sourcing obsidian from late neolithic sites on the great hungarian plain: Preliminary p-XRF compositional results and the socio-cultural implications, Interdiscip. Archaeol. 10 (2019) 113–120, https://doi.org/10.24916/iansa.2019.2.1.

[100] C. Reepmeyer, M. Spriggs, Anggraeni, P. Lape, L. Neri, W.P. Ronquillo, T. Simanjuntak, G. Summerhayes, D. Tanudirjo, A. Tiauzon, Obsidian sources and distribution systems in Island Southeast Asia: New results and implications from geochemical research using LA-ICPMS, J. Archaeol. Sci. 38 (2011) 2995–3005, https://doi.org/10.1016/j.jas.2011.06.023.

[101] R. Torrence, S. Kelloway, P. White, Stemmed Tools, Social Interaction, and Voyaging in Early-Mid Holocene Papua New Guinea, J. Isl. Coast. Archaeol. 8 (2013) 278–310, https://doi.org/10.1080/15564894.2012.761300.

[102] R.H. Tykot, Characterization of the Monte Arci (Sardinia) Obsidian Sources, J. Archaeol. Sci. 24 (1997) 467–479, https://doi.org/10.1006/jasc.1996.0130.

[103] R.H. Tykot, Chemical fingerprinting and source tracing of obsidian: The central mediterranean trade in black gold, Acc. Chem. Res. 35 (2002) 618–627, https://doi.org/10.1021/ar000208p.

[104] N. Craig, R.J. Speakman, R.S. Popelka-Filcoff, M.D. Glascock, J.D. Robertson, M.S. Shackley, M.S. Aldenderfer, Comparison of XRF and PXRF for analysis of archaeological obsidian from southern Perú, J. Archaeol. Sci. 34 (2007) 2012–2024, https://doi.org/10.1016/j.jas.2007.01.015.

[105] M. Orange, F.X. Le Bourdonnec, A. D'Anna, P. Tramoni, C. Lugliè, L. Bellot-Gurlet, A. Scheffers, H. Marchesi, J.L. Guendon, R. Joannes-Boyau, Obsidian economy on the Cauria Plateau (South Corsica, Middle Neolithic): New evidence from Renaghju and I Stantari, Quat. Int. 467 (2018) 323–331, https://doi.org/10.1016/j.quaint.2017.12.033.

[106] E. Frahm, Non-destructive sourcing of bronze age near eastern obsidian artefacts: Redeveloping and reassessing electron microprobe analysis for obsidian sourcing, Archaeometry 54 (2012) 623–642, https://doi.org/10.1111/j.1475-4754.2011.00648.x.

[107] Y. Nishiaki, O. Maeda, T. Kannari, M. Nagai, E. Healey, F. Guliyev, S. Campbell, Obsidian provenance analyses at Göytepe, Azerbaijan: Implications for understanding Neolithic socioeconomies in the southern Caucasus, Archaeometry 61 (2019) 765–782, https://doi.org/10.1111/arcm.12457.

[108] M.R. Iovino, L. Maniscalco, G. Pappalardo, L. Pappalardo, D. Puglisi, F. Rizzo, F.P. Romano, Archaeological volcanic glass from the site of Rocchicella (Sicily, Italy), Archaeometry 50 (2008) 474–494, https://doi.org/10.1111/j.1475-4754.2007.00352.x.

[109] E. Frahm, C.A. Tryon, Origins of Epipalaeolithic obsidian artifacts from Garrod's excavations at Zarzi cave in the Zagros foothills of Iraq, J. Archaeol. Sci. Reports. 21 (2018) 472–485, https://doi.org/10.1016/j.jasrep.2018.08.001.
[110] A.J. Nazaroff, K.M. Prufer, B.L. Drake, Assessing the applicability of portable X-ray fluorescence spectrometry for obsidian provenance research in the Maya lowlands, J. Archaeol. Sci. 37 (2010) 885–895, https://doi.org/10.1016/j.jas.2009.11.019.
[111] E. Frahm, Can I get chips with that? Sourcing small obsidian artifacts down to microdebitage scales with portable XRF, J. Archaeol. Sci. Reports. 9 (2016) 448–467, https://doi.org/10.1016/j.jasrep.2016.08.032.
[112] P. Lopez-García, D.L. Argote, C. Beirnaert, Chemometric analysis of Mesoamerican obsidian sources, Quat. Int. 510 (2019) 100–118, https://doi.org/10.1016/j.quaint.2018.12.032.